Medicine®

CLINICAL CASE REPORT

OPEN

CT, MRI, and ^{18}F-FDG PET/CT Findings in Untreated Pulmonary and Hepatic B-Cell Lymphoma of Mucosa-Associated Lymphoid Tissue (MALT) Over a Five-Year Period

A Case Report

Aisheng Dong, MD, Zhengguang Xiao, MSc, Jianmin Yang, MD, and Changjing Zuo, MD

Abstract: Imaging findings of hepatic lymphoma of mucosa-associated lymphoid tissue (MALT) have been rarely reported before. We present the computed tomography (CT), magnetic resonance imaging (MRI), and fluorine-18-fluorodeoxyglucose (^{18}F-FDG) positron emission tomography (PET)/CT findings in a patient with untreated pulmonary and hepatic MALT lymphoma over a 5-year period.

On the 1st abdominal MRI scan, the hepatic MALT lymphoma showed multiple hepatic subcapsular masses. On FDG PET/CT, these hepatic tumors showed hypodenisty with FDG uptake similar to the liver on early PET images, and higher than liver on delayed PET images. The patient declined to undergo treatment. Fiver year later, the follow-up MRI and FDG PET/CT showed enlargement and confluence of the hepatic tumors with higher FDG uptake than before. The enlarged hepatic tumors had minimal mass effect. In the hepatic lesions, the blood vessels and bile ducts had no distortion or displacement.

The hepatic MALT lymphoma should be taken into consideration when the hepatic tumors have minimal mass effect with the intrahepatic blood vessels and bile ducts normally passing through the tumors. Delayed-time-point FDG PET/CT imaging may be helpful for improving detectability of the hepatic MALT lymphoma.

(*Medicine* 95(12):e3197)

Abbreviations: CT = computed tomography, FDG = fluorodeoxyglucose, MALT = mucosa-associated lymphoid tissue, MRI = magnetic resonance imaging, PET = positron emission tomography, SUV_{max} = maximum standard uptake value.

Editor: Jasna Mihailovic.
Received: February 12, 2016; revised: February 27, 2016; accepted: March 2, 2016.
From the Department of Nuclear Medicine (AD,CZ), Changhai Hospital, Second Military Medical University; Department of Radiology (ZX), Tongren Hospital, Shanghai Jiao Tong University School of Medicine; and Department of Hematology (JY), Changhai Hospital, Second Military Medical University, Shanghai, China.
Correspondence: Changjing Zuo, Department of Nuclear Medicine, Changhai Hospital, 168 Changhai Road, Yangpu District, Shanghai 200433, China (e-mail: 836993813@qq.com).
Jianmin Yang, Department of Hematology, Changhai Hospital, 168 Changhai Road, Yangpu District, Shanghai 200433, China (e-mail: yangjianmin@csco.org.cn).
AD and ZX contributed equally to the article.
The authors have no funding and conflicts of interest to disclose.
Copyright © 2016 Wolters Kluwer Health, Inc. All rights reserved.
This is an open access article distributed under the Creative Commons Attribution- NonCommercial License, where it is permissible to download, share and reproduce the work in any medium, provided it is properly cited. The work cannot be used commercially.
ISSN: 0025-7974
DOI: 10.1097/MD.0000000000003197

INTRODUCTION

Lymphomas of mucosa-associated lymphoid tissue (MALT) are low grade extranodal marginal zone B-cell lymphoma (accounting for approximately 8% of all non-Hodgkin lymphomas) with an indolent course.[1,2] They commonly occur in the gastrointestinal tract and can arise from various nongastrointestinal sites, such as salivary glands, skin, conjunctiva, lung, upper airways, obit, lachrymal gland, liver, breast, pancreas, urogenital tract, kidney, and dura.[2–5] Approximately 34% of cases with MALT lymphoma present with a disseminated disease at diagnosis.[2] Nongastrointestinal MALT lymphoma more frequently occurs simultaneously at different organs than gastrointestinal MALT lymphoma.[4–6] Therefore, accurate staging of MALT lymphoma by radiologic investigation and histopathologic analysis is essential for optimizing treatment. The imaging findings of hepatic MALT lymphoma have been rarely reported before.[7–10] In this paper, we present the computed tomography (CT), magnetic resonance imaging (MRI), and fluorine-18-fluorodeoxyglucose (^{18}F-FDG) positron emission tomography (PET)/CT findings in a patient with untreated pulmonary and hepatic MALT lymphoma over a 5-year period.

CASE REPORT

A 52-year-old female was referred because of 1-month history of chest discomfort. Laboratory tests showed normal a-fetoprotein, carcinoembryonic antigen, carbohydrate antigen 19–9, and carbohydrate antigen 125 levels. Serum hepatitis B virus surface antigen was positive. Chest radiograph and enhanced CT showed multiple peripheral consolidations of the bilateral lungs (Figure 1). CT also showed diffuse right lung-predominant micronodules with peribronchovascular and subpleural distribution (Figure 1). Upper abdominal MRI scan showed multiple hepatic subcapsular masses (Figure 2). These masses showed isointensity on dynamic enhanced MRI. Fluorodeoxyglucose (FDG) PET/CT was performed for further elevation of the patient. Early FDG PET/CT scan (performed 1 hour after injection of tracer) showed increased FDG uptake of the multiple pulmonary consolidations (Figure 3A) with maximum standard uptake value (SUV_{max}) of 5.4. The FDG uptake of hepatic masses (SUV_{max}, 3.5) was similar to the surrounding hepatic parenchyma. The bilateral parotid (SUV_{max}, 1) and submaxillary (SUV_{max}, 2.5) glands were normal. On delayed FDG PET/CT scan (performed 2 hours after injection of tracer), the SUV_{max} of the hepatic masses increased to 4.4. Biopsies of the right pulmonary and hepatic lesions revealed small B-cell lymphocytic hyperplasia in the pulmonary and hepatic parenchyma. B-cell lymphoma was suspected. But the patient declined to undergo any future examination and treatment. Five years

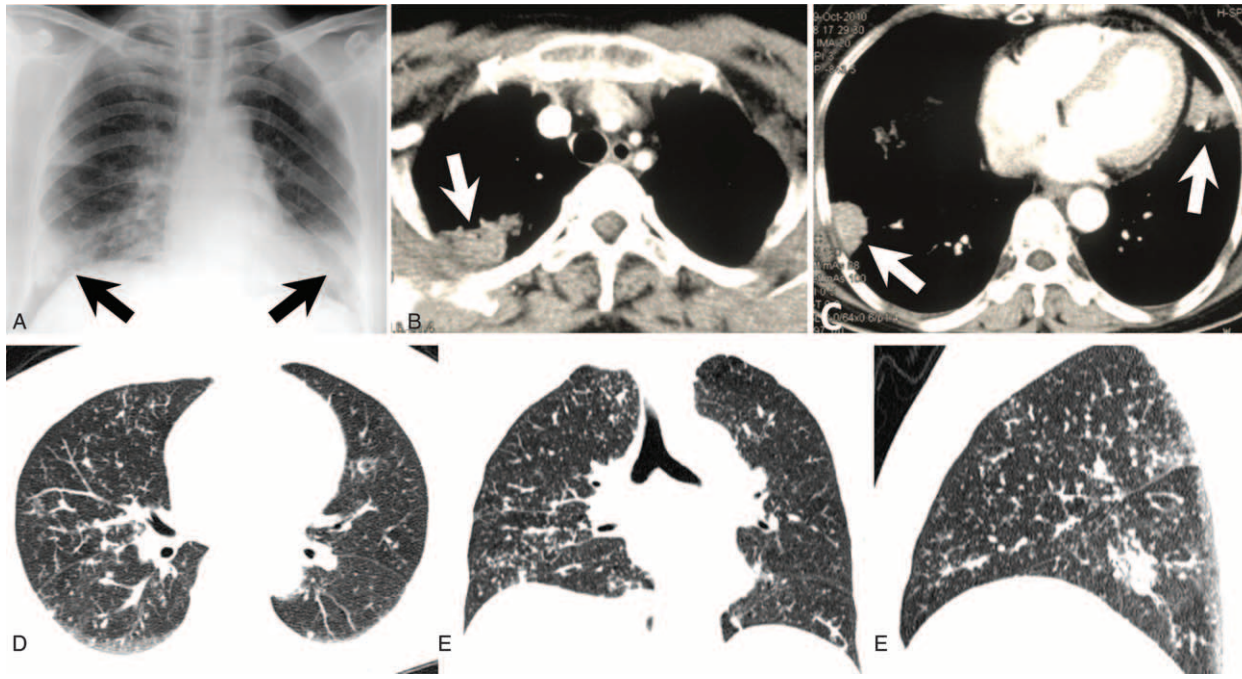

FIGURE 1. Chest radiograph (A) and transverse enhanced computed tomography (CT) (B, C) showed multiple peripheral consolidations (arrows) of the bilateral lungs. Transverse (D), coronal (E), and saggital (F) CT at pulmonary window showed multiple bilateral micronodules with right lung-predominant distribution, and thickening of bronchovascular bundles and interlobular septa.

later, she complained of cough lasting for 20 days. A chest CT was performed showing enlargement of the pulmonary consolidations (Figure 4A–C). Abdominal MRI showed significant enlargement of the hepatic lesions with minimal mass effect (Figure 4D–F). In the hepatic lesions, the blood vessels and bile ducts had no distortion or displacement. FDG PET/CT scan (performed 1 hour after injection of tracer) showed increased FDG uptake of the pulmonary (SUV_{max}, 5.4) and hepatic (SUV_{max}, 4.3) lesions, and bilateral parotid (SUV_{max}, 3.6) and submaxillary (SUV_{max}, 4.1) glands (Figure 5).

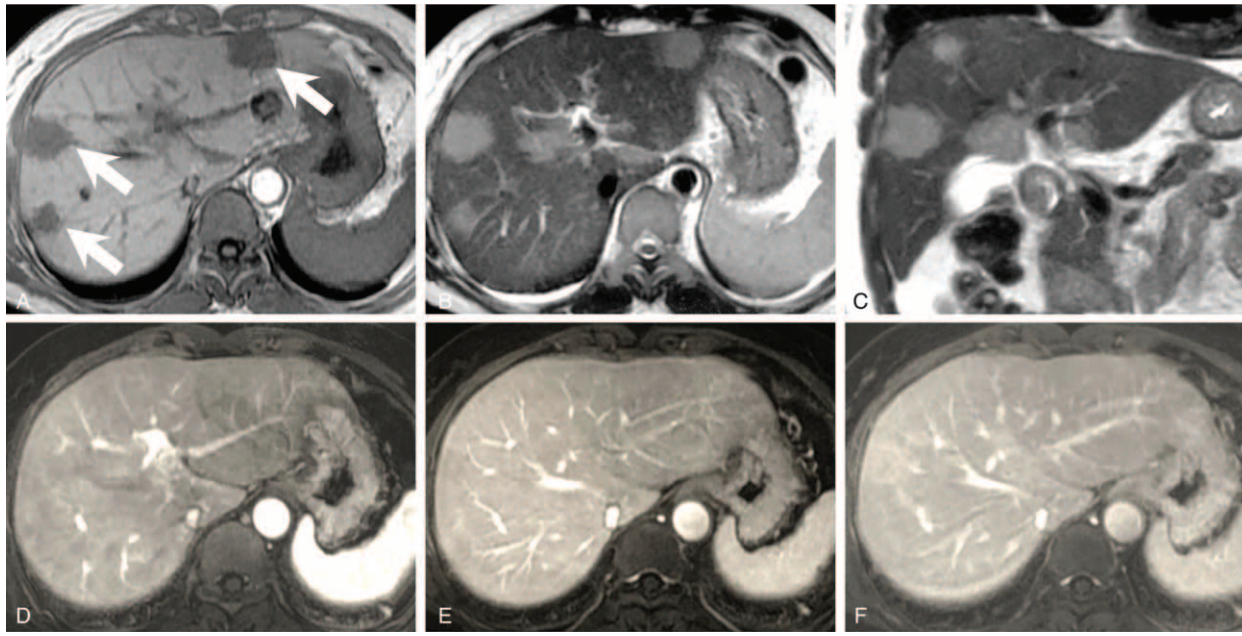

FIGURE 2. Transverse unenhanced T1-weighted magnetic resonance (MR) image (A) showed multiple hypointense hepatic subcapsular masses (arrows). These masses showed hyperintensity on transverse (B) and coronal (C) T2-weighted MR images, and isointensity on enhanced T1-weighted MR images at arterial (D), portal (E), and equilibrium (F) phases.

Copyright © 2016 Wolters Kluwer Health, Inc. All rights reserved.

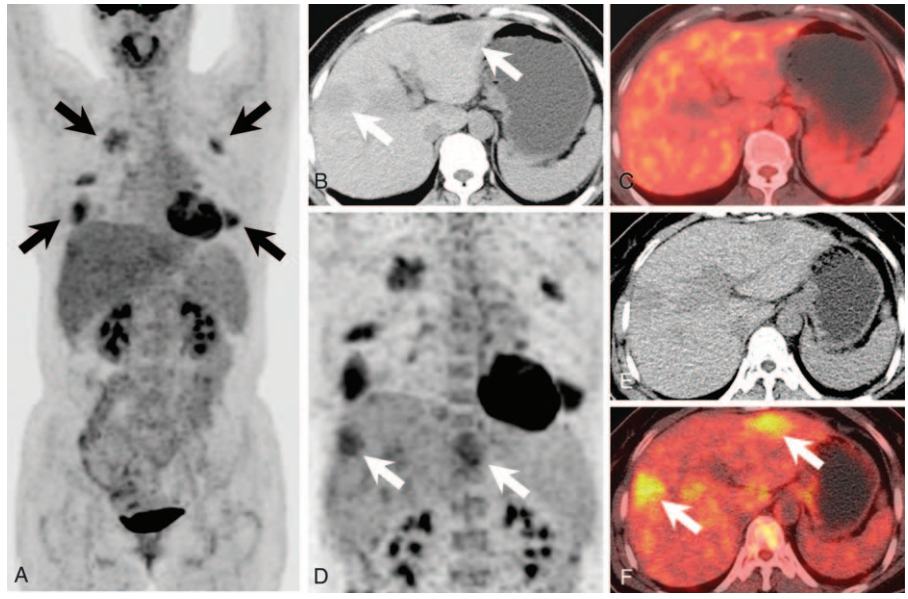

FIGURE 3. Early MIP PET (A) showed multiple hypermetabolic lesions (arrows) (SUV_{max}, 5.4) in the bilateral lungs. The bilateral parotid (SUV_{max}, 1) and submaxillary (SUV_{max}, 2.5) glands were normal. Transverse CT (B) and corresponding fused (C) images showed multiple hypodense hepatic masses (arrows) with SUV_{max} of 3.5. These hepatic masses showed increased FDG uptake (arrows) (SUV_{max}, 4.4) on delayed MIP PET (D), transverse CT (E), and corresponding fused (F) images. CT = computed tomography, FDG = fluorodeoxyglucose, MIP = maximum intensity projection, PET = positron emission tomography, SUV_{max} = maximum standard uptake value.

Ultrasound-guided biopsy of the right pulmonary lesion showed dense proliferation of small lymph cells. Immunohistochemistry staining revealed the lymph cells were positive for CD20, CD79a, and leukocyte common antigen, and negative for CD10 and CD56. Ki-67 staining showed the proportion of the positive tumor cells was about 15%. Bone marrow aspiration and biopsy were normal. Based on these imaging and pathologic findings, the patient was diagnosed with pulmonary and hepatic B-cell MALT lymphoma. Subsequently, the patient underwent chemotherapy with rituximab, cyclophosphamide, doxorubicin, vincristine, and prednisone.

DISCUSSION

The CT features of pulmonary MALT lymphomas include bilateral or unilateral pulmonary nodules, masses or mass-like

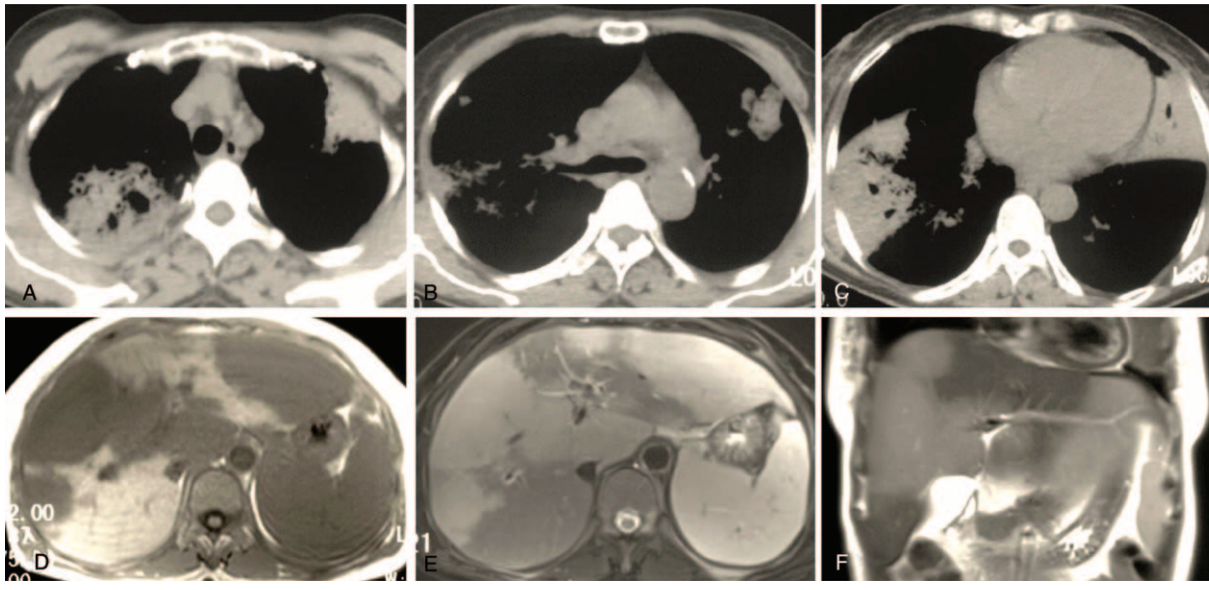

FIGURE 4. Transverse CT (A–C) showed enlargement of the pulmonary lesions with air bronchogram. Transverse T1-weighted MR image (D) showed significant enlargement of the hepatic masses with homogeneous hypointensity. These masses showed homogeneous hyperintensity on transverse (E) and coronal (F) T2-weighted MR images with confluence and minimal mass effect. The spleen became larger than before. CT = computed tomography, MR = magnetic resonance.

Copyright © 2016 Wolters Kluwer Health, Inc. All rights reserved.

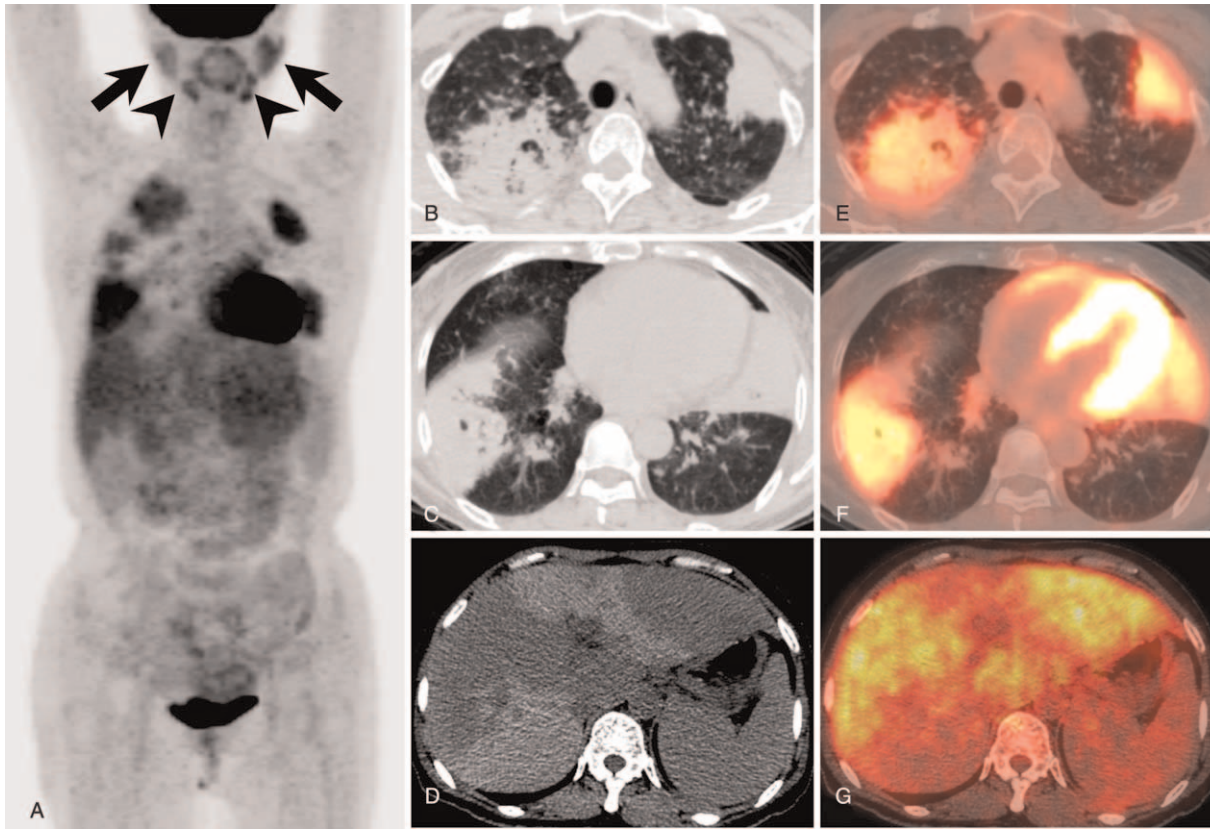

FIGURE 5. MIP PET (A), transverse CT (B–D), and corresponding fused (E–G) images showed increased FDG uptake of the enlarged pulmonary (SUV_{max}, 5.4) and hepatic (SUV_{max}, 4.3) lesions, and bilateral parotid (arrows) (SUV_{max}, 3.6) and submaxillary (arrowheads) (SUV_{max}, 4.1) glands. CT = computed tomography, FDG = fluorodeoxyglucose, MIP = maximum intensity projection, PET = positron emission tomography, SUV_{max} = maximum standard uptake value.

consolidations, with or without air bronchogram.[11–13] Rarely, MALT lymphoma can manifest as mosaic or lymphangitic spread pattern in the lung.[14,15] In this case, the pulmonary MALT lymphoma showed bilateral peripheral consolidations, and diffuse micronodules with lymphangitic distribution. CT or MRI features of hepatic MALT lymphoma are rarely described before.[7–10] Hepatic MALT lymphoma can show unifocal or multifocal nodules or masses with hypodensity on CT, hypointensity on T1-weighted MR images, and hyperintensity on T2-weighted MR images.[7–10]

On FDG PET or PET/CT, MALT lymphoma shows lower FDG uptake compared with the aggressive lymphomas, such as diffuse large B cell lymphoma.[16] The proportion of FDG avid lesions is significantly higher for mass-forming lesions than for superficial lesions in both gastric and nongastric MALT lymphomas, which may be explained by the volume of the tumor.[17] FDG PET/CT is useful for detection of pulmonary MALT lymphoma, which may be due to the minimal background activity of the lung.[17,18] FDG PET/CT may be less useful for the detection of hepatic MALT lymphoma because of relatively higher background activity of the liver.[9,19] We present the changes of CT, MRI, and FDG PET/CT findings in a case with untreated pulmonary and hepatic MALT lymphoma over a 5 years. On the 1st FDG PET/CT scan, the hepatic tumors showed FDG uptake similar to surrounding hepatic parenchyma at early FDG PET images and hypermetabolism at delayed FDG PET images, indicating delayed FDG PET/CT imaging may be more useful for tumor detection. Mayerhoefer et al[19] have also reported that delayed-time-point FDG PET imaging can increase lesion-to-liver and lesion-to-blood contrast than standard-time-point FDG PET, and may improve detectability of MALT lymphoma in liver, stomach, and the small bowl. After 5 years, the pulmonary consolidations remarkably enlarged with air bronchogram, while the FDG uptake degree of the lesions had no significantly increased. The hepatic masses enlarged greatly with confluence and minimal mass effect. In the hepatic lesions, the blood vessels and bile ducts had no distortion or displacement. The FDG uptake of the enlarged hepatic tumors on the second PET/CT scan was higher than that on the 1st PET/CT scan. Unsuspected hypermetabolic lesions in the salivary gland were detected, which may be the new tumor lesions.

In conclusion, the hepatic MALT lymphoma should be taken into consideration when the hepatic tumors have minimal mass effect with the intrahepatic blood vessels and bile ducts normally passing through the tumors. Delayed-time-point FDG PET/CT imaging may be helpful for improving detectability of the hepatic MALT lymphoma.

ETHICAL REVIEW AND CONSENT

Ethical approval was obtained from the Ethics Committee of Changhai Hospital, Shanghai, China. Written informed consent was obtained from the patient for publication of this case report and any accompanying images.

Copyright © 2016 Wolters Kluwer Health, Inc. All rights reserved.

REFERENCES

1. A clinical evaluation of the International Lymphoma Study Group classification of non-Hodgkin's lymphoma. The Non-Hodgkin's Lymphoma Classification Project. *Blood.* 1997;89:3909–3918.
2. Thieblemont C, Berger F, Dumontet C, et al. Mucosa-associated lymphoid tissue lymphoma is a disseminated disease in one third of 158 patients analyzed. *Blood.* 2000;95:802–806.
3. Thieblemont C, Bastion Y, Berger F, et al. Mucosa-associated lymphoid tissue gastrointestinal and nongastrointestinal lymphoma behavior: analysis of 108 patients. *J Clin Oncol.* 1997;15:1624–1630.
4. Zucca E, Conconi A, Pedrinis E, et al. Nongastric marginal zone B-cell lymphoma of mucosa-associated lymphoid tissue. *Blood.* 2003;101:2489–2495.
5. Sretenovic M, Colovic M, Jankovic G, et al. More than a third of non-gastric malt lymphomas are disseminated at diagnosis: a single center survey. *Eur J Haematol.* 2009;82:373–380.
6. Raderer M, Vorbeck F, Formanek M, et al. Importance of extensive staging in patients with mucosa-associated lymphoid tissue (MALT)-type lymphoma. *Br J Cancer.* 2000;83:454–457.
7. Yu YD, Kim DS, Byun GY, et al. Primary hepatic marginal zone B cell lymphoma: a case report and review of the literature. *Indian J Surg.* 2013;75:331–336.
8. Zhong Y, Wang X, Deng M, et al. Primary hepatic mucosa-associated lymphoid tissue lymphoma and hemangioma with chronic hepatitis B virus infection as an underlying condition. *Biosci Trends.* 2014;8:185–188.
9. Hamada T, Kakizaki S, Koiso H, et al. Primary hepatic mucosa-associated lymphoid tissue (MALT) lymphoma. *Clin J Gastroenterol.* 2013;6:150–155.
10. Doi H, Horiike N, Hiraoka A, et al. Primary hepatic marginal zone B cell lymphoma of mucosa-associated lymphoid tissue type: case report and review of the literature. *Int J Hematol.* 2008;88:418–423.
11. Sirajuddin A, Raparia K, Lewis VA, et al. Primary pulmonary lymphoid lesions: radiologic and pathologic findings. *Radiographics.* 2016;36:53–70.
12. King LJ, Padley SP, Wotherspoon AC, et al. Pulmonary MALT lymphoma: imaging findings in 24 cases. *Eur Radiol.* 2000;10:1932–1938.
13. Hayashi D, Devenney-Cakir B, Lee JC, et al. Mucosa-associated lymphoid tissue lymphoma: multimodality imaging and histopathologic correlation. *AJR Am J Roentgenol.* 2010;195:W105–W117.
14. Lee IJ, Kim SH, Koo SH, et al. Bronchus-associated lymphoid tissue (BALT) lymphoma of the lung showing mosaic pattern of inhomogeneous attenuation on thin-section CT: a case report. *Korean J Radiol.* 2000;1:159–161.
15. Kohmo S, Tachibana I, Osaki T, et al. Multiple organ mucosa-associated lymphoid tissue lymphoma presenting with lymphangitic pattern of spread in the lung. *J Thorac Oncol.* 2007;2:1057–1059.
16. Weiler-Sagie M, Bushelev O, Epelbaum R, et al. (18)F-FDG avidity in lymphoma readdressed: a study of 766 patients. *J Nucl Med.* 2010;51:25–30.
17. Park SH, Lee JJ, Kim HO, et al. (18)F-Fluorodeoxyglucose (FDG)-positron emission tomography/computed tomography in mucosa-associated lymphoid tissue lymphoma: variation in (18)F-FDG avidity according to site involvement. *Leuk Lymphoma.* 2015;56:3288–3294.
18. Beal KP, Yeung HW, Yahalom J. FDG-PET scanning for detection and staging of extranodal marginal zone lymphomas of the MALT type: a report of 42 cases. *Ann Oncol.* 2005;16:473–480.
19. Mayerhoefer ME, Giraudo C, Senn D, et al. Does Delayed-Time-Point Imaging Improve 18F-FDG-PET in Patients With MALT Lymphoma?: observations in a series of 13 patients. *Clin Nucl Med.* 2016;41:101–105.

Copyright © 2016 Wolters Kluwer Health, Inc. All rights reserved.